

Human cytomegalovirus IE1 protein alters the higher-order chromatin structure by targeting the acidic patch of the nucleosome

Qianglin Fang^{1,2†}, Ping Chen^{1†}, Mingzhu Wang¹, Junnan Fang^{1,2}, Na Yang^{1,2}, Guohong Li^{1,2*}, Rui-Ming Xu^{1,2*}

¹National Laboratory of Biomacromolecules, Institute of Biophysics, Chinese Academy of Sciences, Beijing, China; ²College of Life Sciences, University of Chinese Academy of Sciences, Beijing, China

Abstract Human cytomegalovirus (hCMV) immediate early 1 (IE1) protein associates with condensed chromatin of the host cell during mitosis. We have determined the structure of the chromatin-tethering domain (CTD) of IE1 bound to the nucleosome core particle, and discovered that the specific interaction between IE1-CTD and the H2A-H2B acidic patch impairs the compaction of higher-order chromatin structure. Our results suggest that IE1 loosens up the folding of host chromatin during hCMV infections.

DOI: [10.7554/eLife.11911.001](https://doi.org/10.7554/eLife.11911.001)

***For correspondence:**

liguohong@sun5.ibp.ac.cn (GL);
rmxu@sun5.ibp.ac.cn (RMX)

†These authors contributed equally to this work

Competing interests: The authors declare that no competing interests exist.

Funding: See page 9

Received: 26 September 2015

Accepted: 21 January 2016

Published: 26 January 2016

Reviewing editor: Patrick Cramer, Max Planck Institute for Biophysical Chemistry, Germany

© Copyright Fang et al. This article is distributed under the terms of the [Creative Commons Attribution License](https://creativecommons.org/licenses/by/4.0/), which permits unrestricted use and redistribution provided that the original author and source are credited.

Introduction

In eukaryotes, nuclear DNA is highly packaged into chromatin by histones. The nucleosome, the basic repeating unit of chromatin, typically assembles 146–147 bp of DNA wrapped around a histone octamer consisting of two copies each of H3, H4, H2A and H2B (Luger et al., 1997a). Nucleosomes connected by linker DNA form a 10-nm array resembling “beads-on-a-string”. The binding of linker histone further compacts the linear array into a more condensed 30-nm chromatin fiber. The interaction between the N-terminal tail of histone H4 and a specific surface region on the neighboring nucleosome termed the “acidic patch” plays crucial roles for the formation of 30-nm chromatin fiber (Dorigo et al., 2004; Luger et al., 1997a; Song et al., 2014). The acidic patch is formed by a number of negatively charged residues of H2A and H2B, including Glu56, Glu61, Glu64, Asp90, Glu91 and Glu92 of H2A, and Glu102 and Glu110 of H2B (Luger et al., 1997a). Several nucleosome-binding proteins have been shown to specifically interact with the acidic patch. Therefore, it has been hypothesized that these proteins may play a role in regulating the higher-order chromatin structure by competing with the H4 N-terminal tails for binding to the acidic patch of the nucleosome (Kalashnikova et al., 2013; McGinty and Tan, 2015).

The 72-kDa immediately early 1 (IE1) protein of human cytomegalovirus (hCMV) plays critical roles in the viral early gene expression and DNA replication (Gawn and Greaves, 2002; MocarSKI et al., 1996). In addition, IE1 has been long known to associate with condensed host chromatin during mitosis (Ahn et al., 1998; Dimitropoulou et al., 2010; Huh et al., 2008; Krauss et al., 2009; Lafemina et al., 1989; Nevels et al., 2004; Reinhardt et al., 2005; Shin et al., 2012; Wilkinson et al., 1998). The chromatin-tethering domain (CTD) located at the very C-terminal end of IE1 (a.a 476–491) is responsible for the association with the mitotic chromosome, specifically through the acidic patch of the nucleosome (Mucke et al., 2014; Reinhardt et al., 2005). However, the molecular mechanism underlying the association and the impact on the structure and function of

eLife digest Most of the DNA in a cell is tightly wrapped around groups of proteins called histones, which gives the impression of beads on a string. These bead-like structures are called nucleosomes, and interactions between histones in different nucleosomes can link one nucleosome to another, to package the DNA into a very condensed form.

Viruses sometimes interact with this condensed DNA; for example, a virus called human cytomegalovirus is known to attach to condensed DNA when cells are preparing to divide. But the consequences of these interactions are not always clear.

Now, Fang, Chen et al. have worked out the three-dimensional structure of a protein from the cytomegalovirus while it is attached to a nucleosome. This structure revealed that the viral protein connects to same part of the histones that otherwise helps pull the nucleosomes together.

Further experiments then compared how the cytomegalovirus protein attaches to nucleosomes with the interaction between nucleosomes and a similar protein from a different virus. Both viral proteins were seen to interact with the same part of the histone protein, but in different ways.

Next, Fang, Chen et al. showed that the DNA is more loosely packed when the cytomegalovirus protein is attached to the nucleosomes. This was not the case for the similar protein from the other virus. The experiments show that small differences in the ways viral proteins interact with condensed DNA can change their effects on DNA packaging. Additionally, these findings may help scientists to better understand how the binding of the cytomegalovirus protein to the nucleosomes might affect this virus's ability to infect or cause illness in humans.

DOI: [10.7554/eLife.11911.002](https://doi.org/10.7554/eLife.11911.002)

host chromatin by IE1 remain to be determined. Here we provide an analysis of the structural basis for the interaction between the CTD of IE1 (IE1-CTD) and the nucleosome core particle (NCP) and explore the impact of their binding on the higher-order structure of chromatin.

Results and discussion

The complex of NCP with an IE1-CTD peptide (a.a. 476–491) was obtained by soaking the peptide into preformed NCP crystals, and a 2.8 Å structure was solved by molecular replacement. The structure shows one molecule of IE1-CTD bound to the NCP (**Figure 1A**; **Figure 1—figure supplement 1**). The presence of only one IE1-CTD peptide in the complex structure is due to the availability of only one side of the NCP surface in the preformed crystal lattice, as in the case of NCP in complex with the latency-associated antigen (LANA) of Kaposi's sarcoma-associated herpes virus (KSHV) (**Barbera et al., 2006**). The IE1-CTD peptide adopts an extended, v-shaped conformation with a short α -helix at its C-terminus. In the complex structure, IE1-CTD is well positioned into the acidic patch of the nucleosome formed by H2A and H2B (**Figure 1A and B**). IE1-CTD contacts histone H2B at two distinct sites, the C-terminal portion of α 1 and the N-terminal half of α C, through van der Waals interaction and intermolecular hydrogen bonds via its mainchain groups. Specifically, the amide and carbonyl groups of Thr480 make hydrogen bonds with the mainchain carbonyl and the sidechain amide groups of Gln44 of H2B (amino acid residue numbering following that in the reference of **Luger et al., 1997a**); the amide and carbonyl groups of Val484 bond the carboxylate group of Glu110 and the nitrogen atom of the imidazole ring of His106, respectively (**Figure 1B**). IE1-CTD contacts histone H2A via a number of sidechain contacts. His481 makes one hydrogen bond with Glu56 of H2A; Thr485 and Ser487 each makes one hydrogen bond with Glu64 of H2A; and Arg486 makes hydrogen bonds with Glu61 on α 2, as well as with Asp90 and Glu92 located on α C of histone H2A. In addition, Met483 of IE1-CTD is placed in a hydrophobic pocket consisting of Leu23, and the aliphatic portion of Glu56 and Tyr57.

The nucleosomal acidic patch is well known for hosting the binding of a number of proteins (**Armache et al., 2011**; **Arnaudo et al., 2013**; **Barbera et al., 2006**; **Kato et al., 2013**; **Makde et al., 2010**; **McGinty et al., 2014**; **Wang et al., 2013**; **Yang et al., 2013**). Most closely related to hCMV IE1 is LANA of KSHV (**Barbera et al., 2006**). The N-terminal CTD of LANA forms a hairpin-like structure that pokes into the acidic patch of the nucleosome (**Figure 1C**). The distinctly folded IE1-CTD and LANA-CTD share certain common features of nucleosome binding. Structural

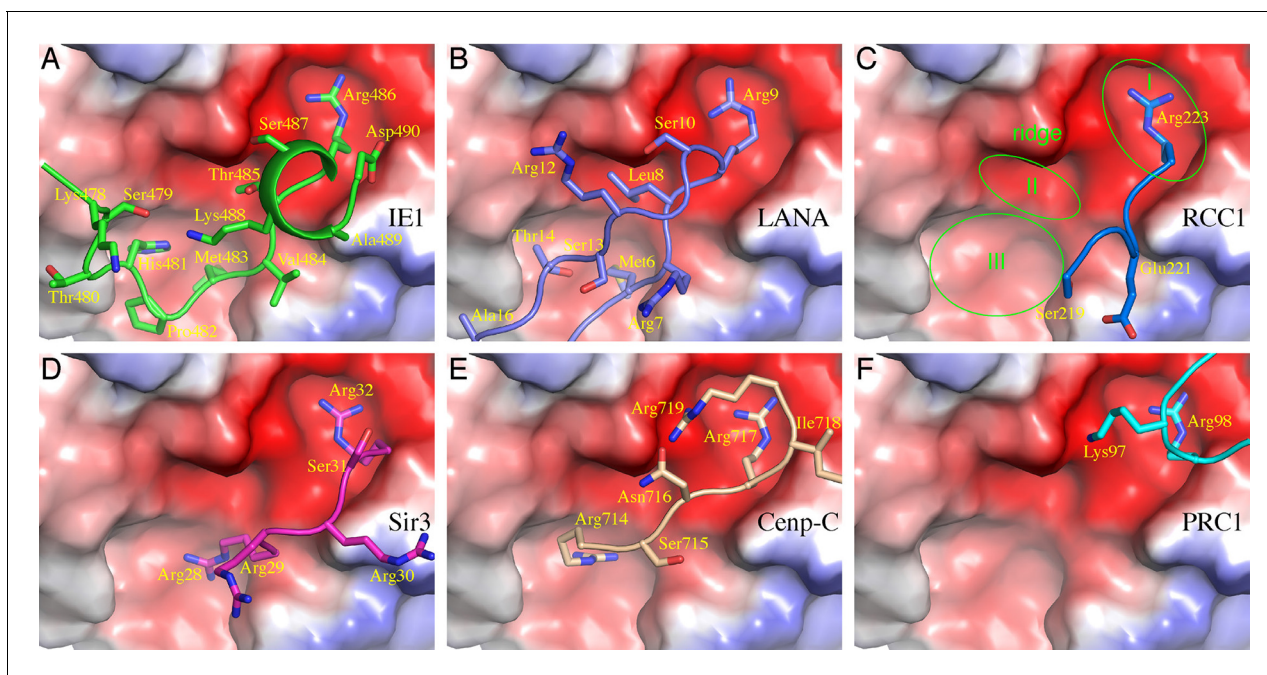


Figure 2. Comparison of protein binding modes to the acidic patch of NCP. All NCP-binding peptides or protein segments, shown in a stick model superimposed onto a cartoon representation of the backbone, were superimposed onto the structure of NCP, shown in a surface representation colored according to electrostatic potential, of the IE1-CTD complex based on alignment of NCP structures. (A) The binding of IE1-CTD to NCP. (B) LANA (PDB id: 1ZLA). (C) RCC1 segment (PDB id: 3MVD). The green ovals indicate distinct binding zones of the acidic patch. The protruding ridge at the junction between zone I and zone II is also labeled. (D) Sir3 (PDB id: 4KUD). (E) CENP-C (PDB id: 4X23). (F) PRC1-RING1B (PDB id: 4R8P).

DOI: 10.7554/eLife.11911.005

H2B. The binding of an arginine in zone I is conserved among all protein-NCP complexes known thus far. Thr485 of IE1 and Leu8 of LANA are bound in zone II, which is unoccupied in other NCP complexes (Figure 2). Main differences accounting for the specific interaction between IE1-CTD and NCP appear to reside in His481, which is bound in zone III and makes a hydrogen bond with Glu56 of H2A, and Thr485, which is bound to zone II and forms a hydrogen bond with Glu64 of H2A. And finally, the binding of the N-terminal segment of IE1-CTD spanning residues 476–480 to $\alpha 1$ of H2B is unique to IE1 (Figure 1B).

To reveal the determinants for the binding specificity of IE1-CTD, we carried out structure-guided mutagenesis of IE1-CTD and histones and analyzed their interactions using isothermal titration calorimetry (ITC). Wild-type IE1-CTD bound to recombinant human NCP with a dissociation constant (K_D) of 0.4 μM , while its mutant lacking the N-terminal segment interacting with $\alpha 1$ of H2B ($\Delta 476$ –480) reduced the nucleosome-binding affinity to a K_D of 12 μM (Figure 3A and B). To put the binding affinities in perspective, an approximately five-fold weaker binding of full-length IE1 than IE1-CTD alone to NCP was observed (Figure 3—figure supplement 1A and B), possibly caused by self-inhibitory effects of other domains in the full-length protein. In comparison, IE1 lacking the CTD showed no detectable binding to NCP (Figure 3—figure supplement 1C). With IE1-CTD, the most severe reduction of binding affinity was seen in the H481A mutant, which has a K_D of 43.4 μM (Figure 3C), while loss of one hydrogen bond by substituting Thr485 with a valine brought the K_D to 11.3 μM (Figure 3D). To gain further insights into the ~hundred-fold reduction of binding affinity introduced by the H481A mutation, we measured the effect of histone H2A mutation on Glu56, which interacts with His481 via hydrogen bonding and Met483 by hydrophobic/van der Waals interaction. ITC measurement shows that the NCP reconstituted with the E56R mutant of H2A, a charge-swap mutant, lowered the binding to IE1-CTD to a level beyond detection (Figure 3E). This change of histone H2A also brought about a conspicuous reduction of the binding of LANA to NCP from a K_D of 0.25 to 23.4 μM (Figure 3F and G). LANA and IE1 share the methionine-mediated interaction with Glu56 in zone III of the acidic patch (Figure 2A and B), and the greater compromise of the binding of IE1-CTD to the H2A-E56R NCP reflects the importance of the His481-Glu56 hydrogen

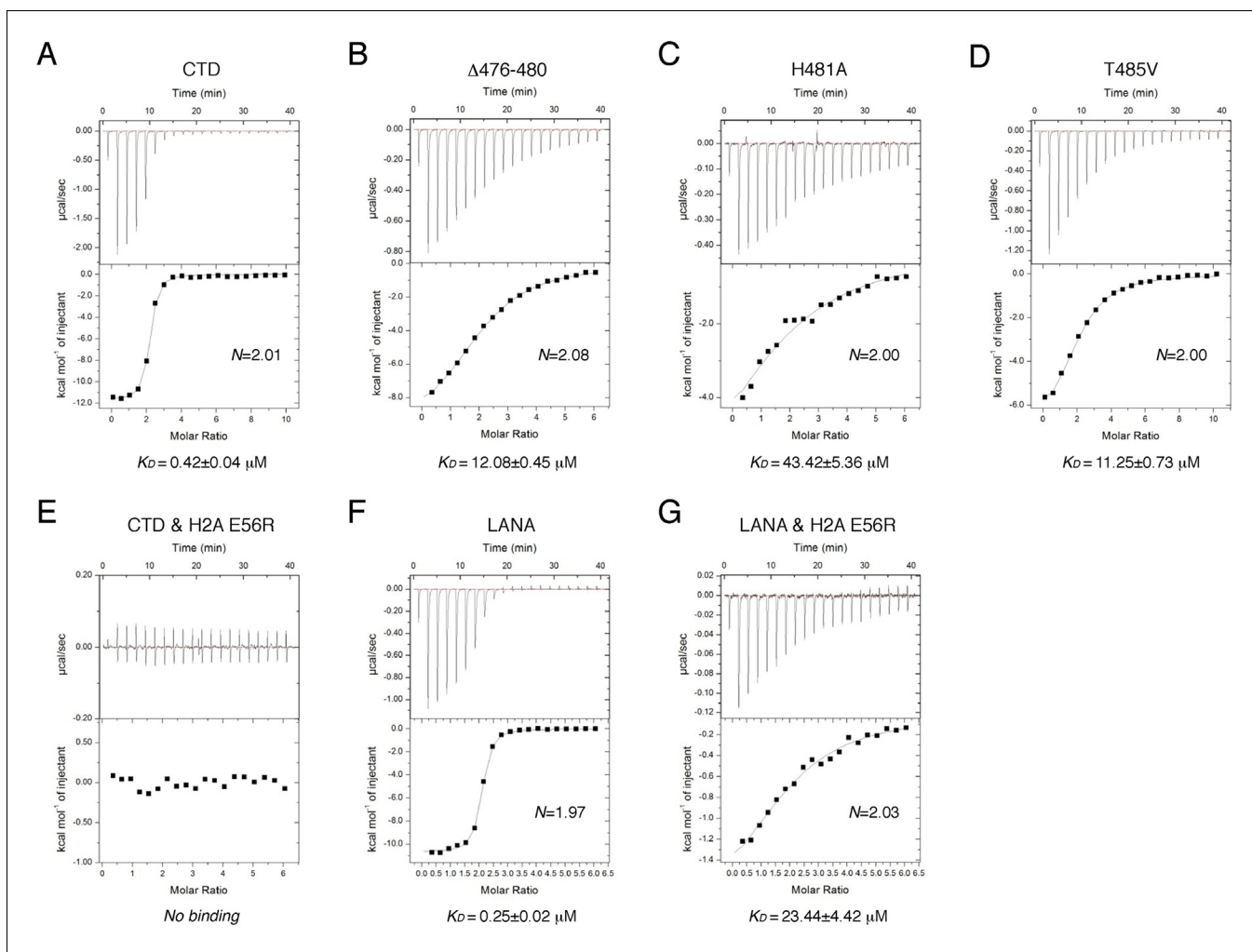


Figure 3. ITC measurements of peptide-NCP binding affinities. (A–G) Raw data and fitting curves of the integrated data for the indicated peptides and NCPs are shown together with the derived K_D values and fitting errors.

DOI: [10.7554/eLife.11911.006](https://doi.org/10.7554/eLife.11911.006)

The following figure supplement is available for figure 3:

Figure supplement 1. Binding of full-length IE1 to NCP.

DOI: [10.7554/eLife.11911.007](https://doi.org/10.7554/eLife.11911.007)

bond in the IE1-NCP complex, as compared to the van der Waals interaction between Thr14 of LANA and Glu56 of histone H2A (**Figure 1B**).

The acidic patch of the nucleosome has been implicated in mediating higher-order chromatin folding via interaction with the N-terminal tail of histone H4 (**Luger et al., 1997a; Schalch et al., 2005**). Our previous cryo-EM structure of 30-nm chromatin fiber reveals that N-terminal tails of histone H4 are involved in inter-nucleosomal contacts between the tetranucleosomal structural units through the acidic patches of adjacent nucleosomes (**Song et al., 2014**). Since IE1-CTD is bound at the acidic patch, it is conceivable that IE1 binding may interfere with proper folding of the 30-nm chromatin fiber. To determine the extent by which the folding of chromatin fiber is affected by IE1 binding, we incubated IE1-CTD with the *in vitro* reconstituted 30-nm chromatin fiber assembled with an array of 12 tandem nucleosomes carrying repeats of 177 bp 601 DNA in the presence of linker histone H1, and analyzed the sample by analytical ultracentrifugation in sedimentation velocity (AUC) (**Song et al., 2014**). The nucleosomal arrays used for reconstituting 30-nm chromatin fiber were highly saturated and homogeneous, as examined by micrococcal nuclease (MNase) digestion and electron microscopy (**Figure 4—figure supplement 1A and B**). For comparison, the same batch of nucleosomal array (without H1) and 30-nm chromatin fiber (with H1) were used in AUC

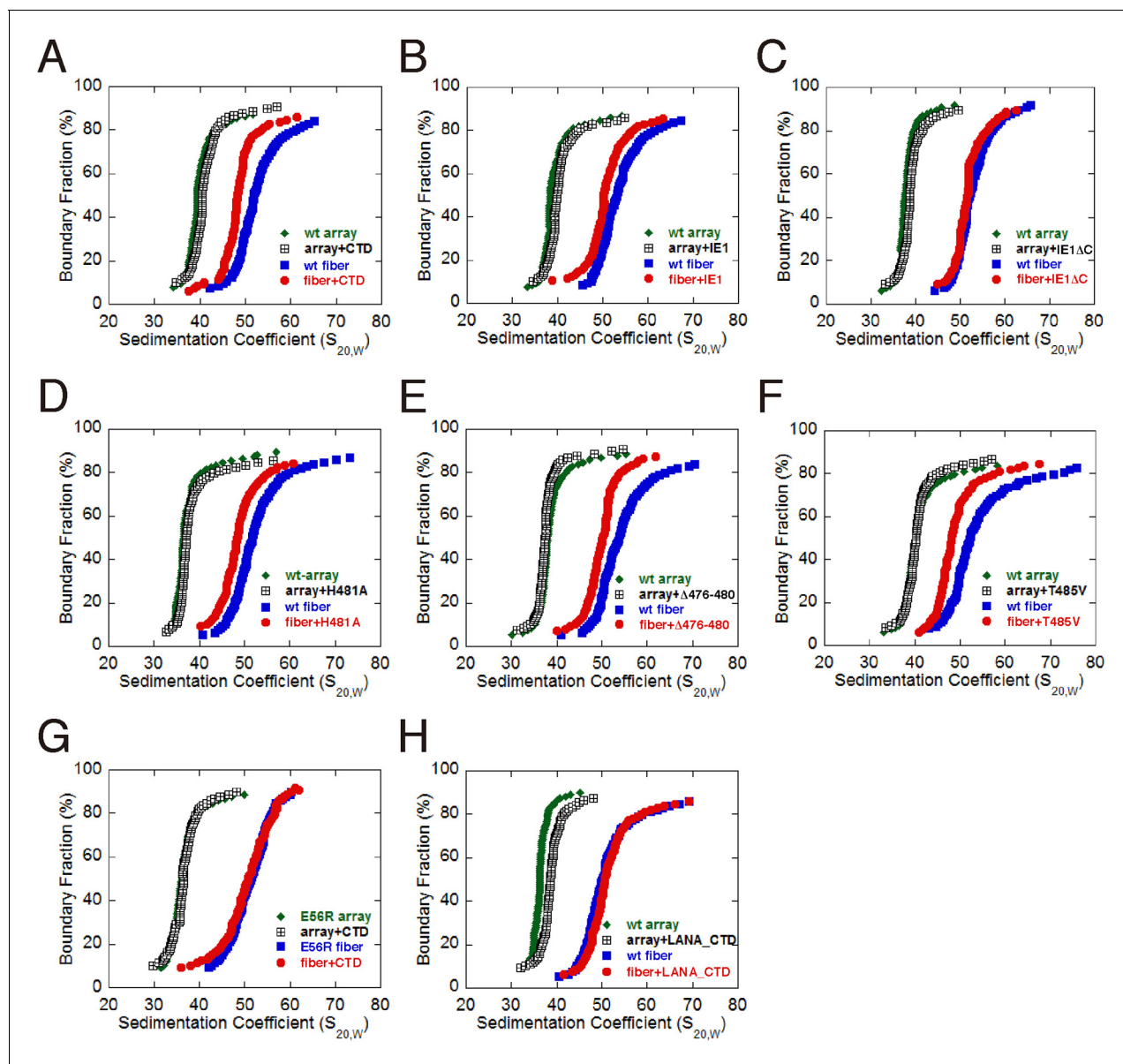


Figure 4. Influence of IE1-CTD on higher-order chromatin structure. (A) AUC analyses showing that IE1-CTD has little effect on the folding of the 10-nm nucleosomal array. Green and black data points represent that of 10-nm nucleosomal arrays in the absence and presence of IE1-CTD, respectively. In contrast, sedimentation profile of the 30-nm chromatin fiber reconstituted in the presence of linker histone H1 (blue squares) was shifted with the addition of IE1-CTD (red dots). (B) Full-length IE1 shares the property of IE1-CTD in selectively altering the folding of the 30-nm chromatin fiber. (C) A truncation variant of IE1 lacking CTD (IE1 Δ C) does not alter chromatin structure. (D–F) Indicated IE1-CTD mutants retain the ability to impact the folding of the 30-nm chromatin fiber. (G) An E56R mutant of histone H2A renders IE1-CTD ineffective in altering the structure of the 30-nm chromatin fiber. (H) LANA-CTD (red dots) does not affect the folding of the 30-nm chromatin fiber. Instead, the 10-nm nucleosome array appears to be slightly affected with the addition of LANA-CTD peptide.

DOI: 10.7554/eLife.11911.008

The following figure supplement is available for figure 4:

Figure supplement 1. Assessment of the quality of reconstituted nucleosomal array.

DOI: 10.7554/eLife.11911.009

analysis. AUC experiments showed that, in the absence of IE1-CTD, the nucleosomal array sedimented with a median sedimentation coefficient S_{ave} (sedimentation coefficient at 50% boundary fraction) of 36 ± 1 S, and the 30-nm chromatin fiber sedimented at 51.5 ± 0.6 S (Figure 3A). In the presence of IE1-CTD, the 10-nm nucleosomal array was unaffected while S_{ave} of the 30-nm chromatin

fiber shifted from 51.5 to 48 S, indicating that the binding of IE1-CTD made the chromatin fiber more loosely folded (**Figure 4A**). It should be emphasized that the IE1-CTD-containing chromatin fiber represents an altered chromatin state different from both the extended 10-nm nucleosomal array and the folded 30-nm chromatin fiber. This chromatin-alteration property of IE1-CTD is shared by the full-length IE1 and fully depends on the presence of CTD (**Figure 4B and C**). Further AUC analyses with IE1-CTD mutants showed that they essentially retained the ability to decondense the 30-nm chromatin fiber, possibly due to their incomplete loss of NCP-binding abilities (**Figure 4D, E and F**). By contrast, chromatin fibers reconstituted with the E56R mutant of histone H2A, previously shown to be unable to interact with IE1-CTD, displayed no alteration of chromatin folding by IE1-CTD (**Figure 4G**). These observations indicate that the binding of IE1-CTD at the acidic patch of the nucleosome modulates the higher-order structure of chromatin. It should be pointed out that not all acidic patch-binding proteins affect chromatin folding, as LANA does not alter the folding of 30-nm chromatin fiber in our AUC analysis (**Figure 4H**).

Our structural analysis revealed that IE1-CTD binds the acidic patch of NCP in a distinct manner. A careful analysis of the landscape of the acidic patch reveals that it can be divided into distinct binding zones that host specific amino acid residues. The conserved binding mode of an arginine in zone I of NCP is important for the association of all NCP-binding partners known to date, while other zones of the acidic patch are involved in differential binding of individual partners. For example, zone III of the acidic patch hosts the binding of His481 of IE1-CTD and Thr14 of LANA, respectively. These two residues interact with Glu56 of histone H2A differently in the structure: while the τ nitrogen of the imidazole ring of His481 makes a hydrogen bond with the carboxylate group of Glu56 of histone H2A at a distance of approximately 2.9 Å, Thr14 of LANA contacts Glu56 of H2A approximately 5 Å away via van der Waals interaction. This difference in peptide-NCP interactions perhaps account for our observations that an E56R mutant affected the binding of IE1-CTD more severely than that with LANA.

For the purpose of dissecting the functions of individual NCP binding partners, one would ideally like to be able to isolate histone mutants that affect the binding of one protein but not others. The most promising such sites appear to lie in zone II and III, as they are less frequently occupied among known NCP binding proteins (**Figure 2**). However, the task is more challenging to distinguish IE1 and LANA bindings, as they both interact with all binding zones of the acidic patches. Nevertheless, the identification of the E56R variant of histone H2A as an IE1-noninteracting mutant has already served as a useful tool for assessing IE1's ability to modulate the higher-order structure of chromatin. Interestingly, this chromatin-modulating activity is not shared by LANA. It was shown previously that the LANA peptide promotes the compaction of nucleosomal arrays, judged by an assay in which the folding of nucleosomal arrays was induced by magnesium ions (**Chodaparambil et al., 2007**). In qualitative agreement with the previous observation, we saw that the addition of LANA made the nucleosomal arrays sedimented slower. Nevertheless, unlike IE1-CTD, LANA has no effect on the preformed H1-containing 30-nm chromatin fiber. There are two possible reasons for the different behavior of LANA, one possibility is that LANA is bound to the chromatin fiber but did not cause any changes to the folding, and the other possibility is that LANA failed to bind 30-nm chromatin fiber. In either case, IE1 and LANA differ in their ability to affect the folding of 30-nm chromatin fiber. The contrasting properties of IE1 and LANA suggest that distinct modes of protein binding to the acidic patch of the nucleosome could exert differential influences to chromatin folding. The discovery of the chromatin modulating activity of IE1 should facilitate further mechanistic understanding of its functions in viral pathogenesis, particularly its impact on the chromatin structure of the host genome, such as transcriptional regulation.

Materials and methods

NCP preparation

To express histones, cDNA fragments encoding *Xenopus laevis* histones H3.3C and H4, H2A type-1 and H2B 1.1, human H3.1 and H4, human H2A type 1-B/E and H2B type 1-J were cloned into pCDFDuet-1 vectors (Novagen) to generate four bicistronic plasmids for co-expression of *Xenopus* and human H3-H4 and H2A-H2B pairs, respectively, in the BL21(DE3)-RIL strain of *E. coli* at 37°C. Bacterial cells overexpressing H3-H4 and H2A-H2B were mixed and lysed together. *Xenopus* and

human histone octamers were then purified as described (Kingston *et al.*, 2011). *Xenopus* NCP was assembled with a 146-bp palindromic DNA fragment derived from human α -satellite DNA according to a described procedure (Luger *et al.*, 1997b). Human NCP was assembled with the 147-bp Widom 601 DNA sequence and the human histone octamer following the same procedure. Human NCP carrying the E56R mutation of histone H2A was generated by mutagenesis using the TaKaRa MutanBEST kit (TaKaRa, China).

Crystallization, data collection, structure determination and refinement

NCP reconstituted with *Xenopus* histones was crystallized by sitting-drop vapor diffusion at 16°C in a condition containing 50 mM sodium cacodylate, pH 6.2, 100 mM magnesium acetate, and 11% 2-methyl-2,4-pentanediol. The co-crystal structure was obtained from a NCP crystal soaked with a chemically synthesized IE1-CTD peptide (a.a. 476–491, SciLight Biotechnology) at 2 mg/ml for 24 hr in a buffer containing 50 mM sodium cacodylate, pH 6.4, 100 mM magnesium acetate, 24% 2-methyl-2,4-pentanediol and 5% trehalose.

X-ray diffraction data were collected at 100K at Beamline BL18U of Shanghai Synchrotron Radiation Facility (SSRF) using a Pilatus 6 M detector at a wavelength of 1.0308 Å, and the data was processed using the HKL2000 package (Otwinowski and Minor, 1997). The structure was solved by molecular replacement with PHASER (McCoy *et al.*, 2007) using the *Xenopus* NCP structure (PDB ID: 1AOI) as the search model. The electron density for the IE1-CTD peptide was clear after refinement with REFMAC (Murshudov *et al.*, 1997) allowing unambiguous building of the IE1-CTD model using COOT (Emsley and Cowtan, 2004). The model was then refined with PHENIX (Adams *et al.*, 2010 COOT). The R_{work} and R_{free} of the final model were 19.5% and 24.4%, respectively. Detailed statistics for crystallographic analyses are shown in Table 1.

Table 1. Statistics of crystallographic analysis.

Data collection statistics	
wavelength (Å)	1.0308
space group	P2 ₁ 2 ₁ 2 ₁
unit cell (Å)	a = 106.70, b = 109.47, c = 181.98
resolution (Å)	30.00–2.80 (2.90–2.80)
R_{merge}	0.133 (0.611)
I/σ	12.5 (3.3)
Completeness (%)	99.9 (100.0)
Total/Unique reflections	346679/52496
Refinement statistics	
$R_{\text{work}}/R_{\text{free}}$	0.195/0.244
rmsd bonds (Å)	0.008
rmsd angles (°)	0.935
No. of Atoms	
Protein	6116
DNA	5982
Peptide	104
Ion	4
Water	230
B factor (Å ²)	
Protein	35.9
DNA	87.8
Peptide	56.9
Ion	47.5
Water	36.0
Ramachandran plot	
favoured	750 (98.7%)
allowed	8 (1.1%)
outlier	2 (0.3%)

DOI: 10.7554/eLife.11911.010

IE1 protein preparation

Plasmids for expressing the full-length hCMV (Towne) IE1 and its truncation variant lacking CTD (IE1 Δ CTD, a.a. 1–475) were obtained from Dr. Michael Nevels (Mucke *et al.*, 2014). Both fragments were expressed as a GST-fusion protein at 16°C in the BL21(DE3)-RIL strain of *E. coli*. They were purified with glutathione-Sepharose resins, followed by cleavage of the GST-tag and further purification with a HiTrap Q HP column (GE Healthcare).

ITC measurement

ITC experiments with IE1-CTD and LANA peptides were performed at 20°C, with the peptide solutions titrated into human NCP solutions in a buffer containing 10 mM Tris-HCl, pH 7.5, and 50 mM NaCl. An NCP concentration of 0.02 mM was used in all experiments, except for the titration of wild-type IE1-CTD into wild-type NCP, in which case 0.018 mM NCP was used. The

peptide concentrations used were, wild-type IE1-CTD at 0.87 mM, T485V at 0.99 mM, and the rest of IE1-CTD mutants and LANA all at 0.59 mM. Detailed procedures follow a protocol published previously (Yang *et al.*, 2013). For the set of ITC experiments involving full-length IE1 and IE1 Δ CTD, a buffer containing 10 mM Hepes, pH 7.4, and 150 mM NaCl was used to minimize background heat generation. Background heat measured through titrating samples from the syringe into the buffer without NCP was subtracted from the integrated data. For comparison, the binding of IE1-CTD to NCP under the same condition was also measured. In the set of experiments, an NCP concentration of 0.015 mM was used, and the concentrations of IE1, IE1 Δ CTD and IE1-CTD used were 0.51, 0.52 and 0.59 mM, respectively.

Chromatin reconstitution and analyses

Recombinant human core histones were prepared as described above. Linker histone H1.4 and DNA templates of 12 tandem 177 bp repeats of the 601 sequence were cloned and purified, and reconstituted into chromatin as previously described (Chen *et al.*, 2013; Dyer *et al.*, 2003; Li *et al.*, 2010; Song *et al.*, 2014).

The reconstituted chromatin samples were subject to AUC analysis in a buffer containing 10 mM HEPES, pH 8.0 and 0.1 mM EDTA. All AUC experiments were performed with nucleosomal array and chromatin fiber concentrations at 0.25 μ M, and peptides/proteins to NCP at 5:1 molar ratio, whenever applicable, on a Beckman Coulter ProteomeLab XL-I, and the data were analyzed using enhanced van Holde-Weischet analysis and the Ultrascan II 9.9 revision 1504 as previously described (Chen *et al.*, 2013).

MNase digestion of nucleosomal arrays follows a procedure described previously (Li *et al.*, 2010). In brief, chromatin sample containing the equivalent of 1 μ g DNA were incubated with micrococcal nuclease (Sigma) in a 50 μ l reaction (10 mM HEPES, pH 7.5, 25 mM KCl, 0.2 mM EDTA, 10% Glycerol and 2 mM CaCl₂) at 37°C for 4 min. The digestion was terminated by addition of 50 μ l stop buffer (200 mM NaCl, 2% SDS, 10 mM EDTA). Each sample were treated with 0.1 mg/ml Proteinase K and reacted at 55°C for 45 min. MNase digested DNA was purified and analyzed on a 1.3% agarose gel.

EM analysis by metal shadowing with tungsten was performed as previously described (Chen *et al.*, 2013). The samples were examined using a FEI Tecnai G2 Spirit 120 kV transmission electron microscope.

Accession codes

The coordinates and diffraction data have been deposited in PDB under the accession code 5E5A.

Acknowledgements

We thank Yuanyuan Chen and Zhenwei Yang for technical support in ITC experiments, staff scientists at beamline BL18U of SSRF for assistance with X-ray data collection, and Dr. Michael Nevels for the generous gift of IE1 expression plasmids. This work was supported by grants from the Ministry of Science and Technology of China (Grant 2015CB856200), Natural Science Foundation of China (Grants 31430018, 31521002, 91219202, 31471218 and 31210103914), and the Strategic Priority Research Program (Grant XDB08010100) of Chinese Academy of Sciences (CAS). PC and NY are also supported by the Youth Innovation Promotion Association of CAS.

Additional information

Funding

Funder	Grant reference number	Author
Ministry of Science and Technology	2015CB856200	Na Yang Guohong Li
National Natural Science Foundation of China	31430018, 31521002, 91219202, 31471218 and 31210103914	Ping Chen Na Yang Guohong Li Rui-Ming Xu

The funders had no role in study design, data collection and interpretation, or the decision to submit the work for publication.

Author contributions

QF, Prepared nucleosomes and proteins, Performed crystallization and ITC measurements, Acquisition of data, Analysis and interpretation of data, Drafting or revising the article; PC, Performed AUC experiments and analyzed data, Acquisition of data, Analysis and interpretation of data, Drafting or revising the article; MW, Collected crystal diffraction data and solved the structure, Edited the manuscript, Acquisition of data, Analysis and interpretation of data; JF, Performed AUC experiments and analyzed data, edited the manuscript, Acquisition of data, Analysis and interpretation of data; NY, Edited the manuscript, Conception and design, Analysis and interpretation of data; GL, R-MX, Conception and design, Analysis and interpretation of data, Drafting or revising the article

Author ORCIDs

Rui-Ming Xu,  <http://orcid.org/0000-0002-6537-4623>

References

- Adams PD, Afonine PV, Bunkóczi G, Chen VB, Davis IW, Echols N, Headd JJ, Hung L-W, Kapral GJ, Grosse-Kunstleve RW, McCoy AJ, Moriarty NW, Oeffner R, Read RJ, Richardson DC, Richardson JS, Terwilliger TC, Zwart PH. 2010. PHENIX: a comprehensive python-based system for macromolecular structure solution. *Acta Crystallographica Section D Biological Crystallography* **66**:213–221. doi: [10.1107/S0907444909052925](https://doi.org/10.1107/S0907444909052925)
- Ahn J-H, Brignole EJ, Hayward GS. 1998. Disruption of PML subnuclear domains by the acidic IE1 protein of human cytomegalovirus is mediated through interaction with PML and may modulate a RING finger-dependent cryptic transactivator function of PML. *Molecular and Cellular Biology* **18**:4899–4913. doi: [10.1128/MCB.18.8.4899](https://doi.org/10.1128/MCB.18.8.4899)
- Armache K-J, Garlick JD, Canzio D, Narlikar GJ, Kingston RE. 2011. Structural basis of silencing: Sir3 BAH domain in complex with a nucleosome at 3.0 Å resolution. *Science* **334**:977–982. doi: [10.1126/science.1210915](https://doi.org/10.1126/science.1210915)
- Arnaudo N, Fernández IS, McLaughlin SH, Peak-Chew SY, Rhodes D, Martino F. 2013. The N-terminal acetylation of Sir3 stabilizes its binding to the nucleosome core particle. *Nature Structural & Molecular Biology* **20**:1119–1121. doi: [10.1038/nsmb.2641](https://doi.org/10.1038/nsmb.2641)
- Barbera AJ, Chodaparambil JV, Kelley-Clarke B, Joukov V, Walter JC, Luger K, Kaye KM. 2006. The nucleosomal surface as a docking station for kaposi's sarcoma herpesvirus LANA. *Science* **311**:856–861. doi: [10.1126/science.1120541](https://doi.org/10.1126/science.1120541)
- Chen P, Zhao J, Wang Y, Wang M, Long H, Liang D, Huang L, Wen Z, Li W, Li X, Feng H, Zhao H, Zhu P, Li M, Wang Q.-f., Li G. 2013. H3.3 actively marks enhancers and primes gene transcription via opening higher-ordered chromatin. *Genes & Development* **27**:2109–2124. doi: [10.1101/gad.222174.113](https://doi.org/10.1101/gad.222174.113)
- Chodaparambil JV, Barbera AJ, Lu X, Kaye KM, Hansen JC, Luger K. 2007. A charged and contoured surface on the nucleosome regulates chromatin compaction. *Nature Structural & Molecular Biology* **14**:1105–1107. doi: [10.1038/nsmb1334](https://doi.org/10.1038/nsmb1334)
- Dimitropoulou P, Caswell R, McSharry BP, Greaves RF, Spandidos DA, Wilkinson GWG, Sourvinos G. 2010. Differential relocation and stability of PML-body components during productive human cytomegalovirus infection: detailed characterization by live-cell imaging. *European Journal of Cell Biology* **89**:757–768. doi: [10.1016/j.ejcb.2010.05.006](https://doi.org/10.1016/j.ejcb.2010.05.006)
- Dorigo B, Schalch T, Kulangara A, Duda S, Schroeder RR, Richmond TJ. 2004. Nucleosome arrays reveal the two-start organization of the chromatin fiber. *Science* **306**:1571–1573. doi: [10.1126/science.1103124](https://doi.org/10.1126/science.1103124)
- Dyer PN, Edayathumangalam RS, White CL, Bao Y, Chakravarthy S, Muthurajan UM, Luger K. 2003. Reconstitution of nucleosome core particles from recombinant histones and DNA. *Methods Enzymol* **375**:23–44. doi: [10.1016/S0076-6879\(03\)75002-2](https://doi.org/10.1016/S0076-6879(03)75002-2)
- Emsley P, Cowtan K. 2004. Coot: model-building tools for molecular graphics. *Acta Crystallographica Section D Biological Crystallography* **60**:2126–2132. doi: [10.1107/S0907444904019158](https://doi.org/10.1107/S0907444904019158)
- Gawn JM, Greaves RF. 2002. Absence of IE1 p72 protein function during low-multiplicity infection by human cytomegalovirus results in a broad block to viral delayed-early gene expression. *Journal of Virology* **76**:4441–4455. doi: [10.1128/JVI.76.9.4441-4455.2002](https://doi.org/10.1128/JVI.76.9.4441-4455.2002)
- Huh YH, Kim YE, Kim ET, Park JJ, Song MJ, Zhu H, Hayward GS, Ahn J-H. 2008. Binding STAT2 by the acidic domain of human cytomegalovirus IE1 promotes viral growth and is negatively regulated by SUMO. *Journal of Virology* **82**:10444–10454. doi: [10.1128/JVI.00833-08](https://doi.org/10.1128/JVI.00833-08)
- Kalashnikova AA, Porter-Goff ME, Muthurajan UM, Luger K, Hansen JC. 2013. The role of the nucleosome acidic patch in modulating higher order chromatin structure. *Journal of the Royal Society Interface* **10**:20121022. doi: [10.1098/rsif.2012.1022](https://doi.org/10.1098/rsif.2012.1022)

- Kato H**, Jiang J, Zhou B-R, Rozendaal M, Feng H, Ghirlando R, Xiao TS, Straight AF, Bai Y. 2013. A conserved mechanism for centromeric nucleosome recognition by centromere protein CENP-c. *Science* **340**:1110–1113. doi: [10.1126/science.1235532](https://doi.org/10.1126/science.1235532)
- Kingston IJ**, Yung JSY, Singleton MR. 2011. Biophysical characterization of the centromere-specific nucleosome from budding yeast. *Journal of Biological Chemistry* **286**:4021–4026. doi: [10.1074/jbc.M110.189340](https://doi.org/10.1074/jbc.M110.189340)
- Krauss S**, Kaps J, Czech N, Paulus C, Nevels M. 2009. Physical requirements and functional consequences of complex formation between the cytomegalovirus IE1 protein and human STAT2. *Journal of Virology* **83**:12854–12870. doi: [10.1128/JVI.01164-09](https://doi.org/10.1128/JVI.01164-09)
- Lafemina RL**, Pizzorno MC, Mosca JD, Hayward GS. 1989. Expression of the acidic nuclear immediate-early protein (iE1) of human cytomegalovirus in stable cell lines and its preferential association with metaphase chromosomes. *Virology* **172**:584–600. doi: [10.1016/0042-6822\(89\)90201-8](https://doi.org/10.1016/0042-6822(89)90201-8)
- Li G**, Margueron R, Hu G, Stokes D, Wang Y-H, Reinberg D. 2010. Highly compacted chromatin formed in vitro reflects the dynamics of transcription activation in vivo. *Molecular Cell* **38**:41–53. doi: [10.1016/j.molcel.2010.01.042](https://doi.org/10.1016/j.molcel.2010.01.042)
- Luger K**, Mäder AW, Richmond RK, Sargent DF, Richmond TJ. 1997a. Crystal structure of the nucleosome core particle at 2.8 Å resolution. *Nature* **389**:251–260. doi: [10.1038/38444](https://doi.org/10.1038/38444)
- Luger K**, Rechsteiner TJ, Flaus AJ, Waye MMY, Richmond TJ. 1997b. Characterization of nucleosome core particles containing histone proteins made in bacteria. *Journal of Molecular Biology* **272**:301–311. doi: [10.1006/jmbi.1997.1235](https://doi.org/10.1006/jmbi.1997.1235)
- Makde RD**, England JR, Yennawar HP, Tan S. 2010. Structure of RCC1 chromatin factor bound to the nucleosome core particle. *Nature* **467**:562–566. doi: [10.1038/nature09321](https://doi.org/10.1038/nature09321)
- McCoy AJ**, Grosse-Kunstleve RW, Adams PD, Winn MD, Storoni LC, Read RJ. 2007. Phaser crystallographic software. *Journal of Applied Crystallography* **40**:658–674. doi: [10.1107/S0021889807021206](https://doi.org/10.1107/S0021889807021206)
- McGinty RK**, Henrici RC, Tan S. 2014. Crystal structure of the PRC1 ubiquitylation module bound to the nucleosome. *Nature* **514**:591–596. doi: [10.1038/nature13890](https://doi.org/10.1038/nature13890)
- McGinty RK**, Tan S. 2015. Nucleosome structure and function. *Chemical Reviews* **115**:2255–2273. doi: [10.1021/cr500373h](https://doi.org/10.1021/cr500373h)
- Mocarski ES**, Kemble GW, Lyle JM, Greaves RF. 1996. A deletion mutant in the human cytomegalovirus gene encoding IE1(491aa) is replication defective due to a failure in autoregulation. *Proceedings of the National Academy of Sciences of the United States of America* **93**:11321–11326. doi: [10.1073/pnas.93.21.11321](https://doi.org/10.1073/pnas.93.21.11321)
- Mucke K**, Paulus C, Bernhardt K, Gerrer K, Schon K, Fink A, Sauer E-M, Asbach-Nitzsche A, Harwardt T, Kieninger B, Kremer W, Kalbitzer HR, Nevels M. 2014. Human cytomegalovirus major immediate early 1 protein targets host chromosomes by docking to the acidic pocket on the nucleosome surface. *Journal of Virology* **88**:1228–1248. doi: [10.1128/JVI.02606-13](https://doi.org/10.1128/JVI.02606-13)
- Murshudov GN**, Vagin AA, Dodson EJ. 1997. Refinement of macromolecular structures by the maximum-likelihood method. *Acta Crystallographica Section D Biological Crystallography* **53**:240–255. doi: [10.1107/S0907444996012255](https://doi.org/10.1107/S0907444996012255)
- Nevels M**, Brune W, Shenk T. 2004. SUMOylation of the human cytomegalovirus 72-kilodalton IE1 protein facilitates expression of the 86-kilodalton IE2 protein and promotes viral replication. *Journal of Virology* **78**:7803–7812. doi: [10.1128/JVI.78.14.7803-7812.2004](https://doi.org/10.1128/JVI.78.14.7803-7812.2004)
- Otwinowski Z**, Minor W. 1997. Processing of x-ray diffraction data collected in oscillation mode. *Macromolecular Crystallography, Pt A* **276**:307–326. doi: [10.1016/S0076-6879\(97\)76066-X](https://doi.org/10.1016/S0076-6879(97)76066-X)
- Reinhardt J**, Smith GB, Himmelheber CT, Azizkhan-Clifford J, Mocarski ES. 2005. The carboxyl-terminal region of human cytomegalovirus IE1491aa contains an acidic domain that plays a regulatory role and a chromatin-tethering domain that is dispensable during viral replication. *Journal of Virology* **79**:225–233. doi: [10.1128/JVI.79.1.225-233.2005](https://doi.org/10.1128/JVI.79.1.225-233.2005)
- Schalch T**, Duda S, Sargent DF, Richmond TJ. 2005. X-ray structure of a tetranucleosome and its implications for the chromatin fibre. *Nature* **436**:138–141. doi: [10.1038/nature03686](https://doi.org/10.1038/nature03686)
- Shin HJ**, Kim Y-E, Kim ET, Ahn J-H. 2012. The chromatin-tethering domain of human cytomegalovirus immediate-early (iE) 1 mediates associations of IE1, PML and STAT2 with mitotic chromosomes, but is not essential for viral replication. *Journal of General Virology* **93**:716–721. doi: [10.1099/vir.0.037986-0](https://doi.org/10.1099/vir.0.037986-0)
- Song F**, Chen P, Sun D, Wang M, Dong L, Liang D, Xu R-M, Zhu P, Li G. 2014. Cryo-EM study of the chromatin fiber reveals a double helix twisted by tetranucleosomal units. *Science* **344**:376–380. doi: [10.1126/science.1251413](https://doi.org/10.1126/science.1251413)
- Wang F**, Li G, Altaf M, Lu C, Currie MA, Johnson A, Moazed D. 2013. Heterochromatin protein Sir3 induces contacts between the amino terminus of histone H4 and nucleosomal DNA. *Proceedings of the National Academy of Sciences of the United States of America* **110**:8495–8500. doi: [10.1073/pnas.1300126110](https://doi.org/10.1073/pnas.1300126110)
- Wilkinson GM**, Kelly C, Sinclair JH, Rickards C. Rickards C1998. Disruption of PML-associated nuclear bodies mediated by the human cytomegalovirus major immediate early gene product. *Journal of General Virology* **79**:1233–1245. doi: [10.1099/0022-1317-79-5-1233](https://doi.org/10.1099/0022-1317-79-5-1233)
- Yang D**, Fang Q, Wang M, Ren R, Wang H, He M, Sun Y, Yang N, Xu R-M. 2013. Nalpa-acetylated Sir3 stabilizes the conformation of a nucleosome-binding loop in the BAH domain. *Nature Structural & Molecular Biology* **20**:1116–1118. doi: [10.1038/nsmb.2637](https://doi.org/10.1038/nsmb.2637)